Pure Appl. Chem., Vol. 83, No. 11, pp. 2089–2106, 2011.
doi:10.1351/PAC-CON-11-04-03

Porous carbon layers for counter electrodes in dye-sensitized solar cells: Recent advances and a new screen-printing method*

Seigo Ito‡ and Yuuki Mikami

Department of Electrical Engineering and Computer Sciences, Graduate School of Engineering, University of Hyogo, 2167 Shosha, Himeji, Hyogo 671-2280, Japan

Abstract: We review the recent literature on carbon catalyst layers for dye-sensitized solar cells (DSCs), and then report an improved fabrication method for screen-printed carbon counter electrodes. The carbon-printing ink was prepared by mixing carbon black, TiO_2 nanoparticles, α-terpineol, and ethyl cellulose using a mortar, an ultrasonic homogenizer, and a rotary evaporator. Scanning electron microscopy (SEM) showed that the resulting screen-printed carbon layers were flatter and smoother at nano- and micro-scales than a carbon layer prepared using water-based ink. The photovoltaic performance of the screen-printed catalyst layers was similar to the photoenergy conversion of platinum counter electrodes. The highest cell efficiency with a carbon counter electrode was 7.11 % at a light intensity of 100 mW cm^{-2}.

Keywords: carbon nanotubes; dye-sensitized solar cells; platinum; porous carbon; scanning electron microscopy (SEM); screen printing.

INTRODUCTION AND OVERVIEW

Dye-sensitized solar cells (DSCs), which can be fabricated using a non-vacuum printing system, have attracted academic and industrial attention because of the demand for cost-effective, renewable energy sources. The basic DSC structure is: transparent conducting oxide electrode (TCO)/porous TiO_2/dye/electrolyte/Pt/conducting substrate (TCO or metal) (Fig. 1). A catalytic layer is necessary for DSCs, in order to reduce I_3^- to I^- in the electrolyte. Although DSCs have a short energy payback time,

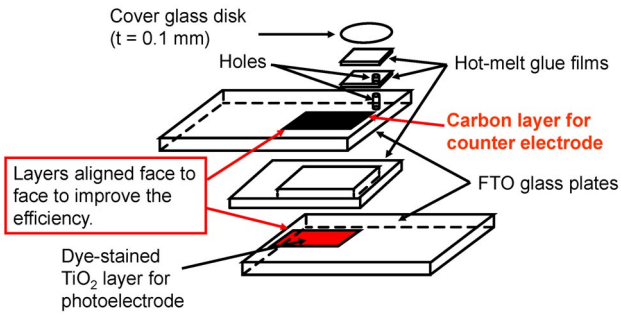

Fig. 1 Structure of DSCs using carbon counter electrode.

*Paper based on a presentation made at the International Conference on Nanomaterials and Nanotechnology (NANO-2010), Tiruchengode, India, 13–16 December 2010. Other presentations are published in this issue, pp. 1971–2113.

‡Corresponding author: Tel./Fax: +81-79-267-4858; E-mail: itou@eng.u-hyogo.ac.jp

a further reduction in cost is necessary. Platinum, carbon, and some kinds of conducting polymers [poly(3,4-ethylenedioxythiophene) (PEDOT), polyaniline, etc.] can be used as the catalytic layer. In order to reduce the cost, Kay and Grätzel replaced the platinum counter electrodes with carbon electrodes [1].

This report summarizes the recent progress in carbon counter electrodes for DSCs in Tables 1, 2, and 3 [1–56], although it excludes pure polymer counter electrodes (PEDOT:PSS [57], etc.) without carbon powders. PEDOT:PSS polymer is very expensive and therefore not suitable for cost-effective DSCs. In addition, such electron-conducting polymers can be unstable to the iodide electrolyte, because of deterioration of the polymer double bonds and the dissolution of the polymers into the electrolyte. In contrast, carbon counter electrodes remained stable for 3000 h at 60 °C, and for 2.5 years under outdoor working conditions [39]. This may be because the DSCs were monolithic structures [1,2,22,23] and the sintered carbon counter electrodes did not contain polymer residues. Hence, it was concluded that carbon counter electrodes are very stable and suitable for industrial applications. In 2008, Murakami and Grätzel published a review of the literature on non-platinum counter electrodes for DSCs [7], and subsequently, 40 papers on this subject have been published.

Table 1 Reported carbon counter electrodes for DSCs prepared by doctor-blade coating method (CNT: carbon nanotube, *d*: diameter, *t*: thickness, Sc: specific surface area, FTO: F-doped SnO_2, ITO: indium tin oxide, PEN: polyethylene naphthalate).

Ref. number	Year	Substrates	Annealing conditions	Materials	Photoenergy conversion efficiency of carbon (or Pt) counter electrodes (%)		
					Carbon (C)	Pt	Ratio: (C)/(Pt)
1	1996	Porous TiO_2/ZrO_2 electrode (monolithic structure)	450 °C for 10 min	Graphite + carbon black (20 wt % of TiO_2) + TiO_2 colloid (15 wt % of TiO_2)	6.67	No data	–
2	1999	Porous TiO_2/ZrO_2 electrode (monolithic structure)	No details (in references)	Soot (20 %) + graphite (80 %)	2.5	5.8	0.43
3	2003	FTO/glass	180 °C for 1 h	Powder carbon (0.2 g) + carbon black (0.4 g) + water (16 mg) + ethanol (8 mL) + carboxylmethyl cellulose (0.24 g)	3.89	4.3	0.90
4	2006	FTO/glass	450 °C for 30 min	Carbon powder (130 mg, Printex L, Degussa) + TiO_2 colloid (0.2 mL) + water (0.4 mL) + Triton X-100 (0.2 mL, 10 % aqueous solution)	9.1	No data	–
5	2007	FTO/glass	250 °C for 1 h	Nano-size carbon (d = 30 nm, Sc = 100 m^2/g) + organic binder + water	6.73	7.26	0.93
				Micro-size carbon (d = 2–12 μm, Sc = 0.4 m^2/g) + organic binder + water	1.87	7.26	0.26

(*continues on next page*)

Table 1 (*Continued*).

Ref. number	Year	Substrates	Annealing conditions	Materials	Photoenergy conversion efficiency of carbon (or Pt) counter electrodes (%)		
					Carbon (C)	Pt	Ratio: (C)/(Pt)
6	2008	FTO/glass	175 °C for 1 h	Carbon (2 g, d = 10 μm, Sc = 1100 m^2/g, Bellfine APK 11001) + carbon black (0.4 g, Sc = 68 m^2/g, Denki Kagaku Kougyo Co. Ltd., Denka Black) + water (16 mL) + ethanol (8 mL) + carboxymethyl cellulose (CMC) ammonium salt (0.25 g, Wako Pure Chemical Industries, Ltd. SDE2048)	0.52	No data	No data
7	2008	Stainless (SUS-316)	450 °C for 30 min	Carbon powder (130 mg, Printex L, Degussa) + TiO_2 colloid (0.2 mL) + water (0.4 mL) + Triton X-100 (0.2 mL, 10 % aqueous solution)	9.15	11.18	0.82
8	2008	FTO/glass	250 °C for 1 h	Carbon powder (d = 40 nm) + organic binder + water	4.23	5.26	0.80
9	2008	FTO/glass	175 °C for 1 h	Carbon powder (2.0 g, Belfine APK1101, d = 10 μm, Sc = 1100 m^2/g) + carbon black (0.4g, Sc = 68 m^2/g) + water (16 mL) + ethanol (8 mL) + carboxymethyl cellulose ammonium salt (0.25g)	2.85	No data	–
10	2008	FTO/glass	250 °C for 1 h	Carbon powder (d = 30 nm) + organic binder	7.56	7.61	0.99
11	2009	FTO/glass	500 °C for 30 min.	Microporous carbon from cornstalks (0.1 g) + ethyl cellulose (0.25g) + α-terpineol (0.75 mL) + carbon black (0.015 g, Vulcan XC-72, 250 m^2/g) + TiO_2 (0.01 g, P25, Degussa)	7.36	7.81	0.94
				Ethyl cellulose + α-terpineol + carbon black (Vulcan XC-72, 250 m^2/g) + TiO_2 (P25, Degussa)	4.81	7.81	0.62
12	2009	FTO/glass	400 °C for 20 min.	Mesoporous carbon (from triblock copolymer F127, 150 mg) + TiO_2 colloid (10 wt %, 0.2 mL) + water (0.3 mL) + Triton X-100 (10 %, 0.1 mL)	6.18	6.26	0.99

(*continues on next page*)

Table 1 (*Continued*).

Ref. number	Year	Substrates	Annealing conditions	Materials	Photoenergy conversion efficiency of carbon (or Pt) counter electrodes (%)		
					Carbon (C)	Pt	Ratio: (C)/(Pt)
13	2009	Flexible graphite sheets (t = 0.2 mm, density = 0.03 g/m^2)	Specified temperature for 60 min	Activated carbon (0.4 g, Sc = 1958 m^2/g, d = 1–10 μm) + carbon black (0.1 g, d = 30 nm, 77 m^2/g) + α-terpineol (4g) + SnO_2 (0.1 g, d = 10 nm)	6.46	6.37	1.01
		FTO/glass		Activated carbon (0.4 g, Sc = 1958 m^2/g, d = 1–10 μm) + carbon black (0.1 g, d = 30 nm, 77 m^2 g) + -terpineol (4 g) + SnO_2 (0.1 g, d = 10 nm)	6.17	6.37	0.97
14	2009	FTO/glass	120 °C for 1 h.	Active carbon (0.4 g, Sc = 1958 m^2/g) + carbon black (0.1 g, Sc = 77 m^2/g, d = 30 nm) + $SnCl_4$ (4 mL)	6.1	7	0.87
15	2009	FTO/glass	180 °C for 1 h	Carbon black (300 mg) + hydroxyethyl cellulose (30 mg) + water (2 mL) + ethanol (2 mL)	3.76	6.63	0.57
16	2010	FTO/glass	400 °C for 5 min	Hollow macroporous core/ mesoporous shell carbon (100 mg) + ethanol (10 mL)	7.56	7.79	0.97
				Ordered mesoporous carbon (100 mg, named as CMK-3) + ethanol (10 mL)	7.03	7.79	0.90
				Activated carbon (100 mg, Duksan Pharm. Co., Korea) + ethanol (10 mL)	6.24	7.79	0.80
17	2010	ITO/PEN	140 °C for 4 h + UV/O_3 treatment for 3 min	Mesoporous carbon (20 mg) + TiO_2 colloid (0.1 mL, 2 wt %) + tetrabutyl titanate (1.5 mL, 0.1 mol/L, in 1-butanol solution)	6.07	7.07	0.86
18	2010	FTO/glass	No details	Mesoporous carbon (from triblock copolymer F127, 130 mg) + TiO_2 colloid (10 wt %, 0.2 mL) + water (0.3 mL) + Triton X-100 (10 %, 0.1 mL)	6.18	6.25	0.99

(*continues on next page*)

Table 1 (*Continued*).

Ref. number	Year	Substrates	Annealing conditions	Materials	Photoenergy conversion efficiency of carbon (or Pt) counter electrodes (%)		
					Carbon (C)	Pt	Ratio: (C)/(Pt)
19	2010	FTO/glass	60 °C for 24 h	TiN-CNT + ethanol + carboxymethyl cellulose	5.41	5.58	0.97
				CNT + ethanol + carboxymethyl cellulose	3.53	5.58	0.63
				TiN + ethanol + carboxymethyl cellulose	2.1	5.58	0.38
20	2010	FTO/glass	No details	CNT micro-balls + α-terpineol + ethyl cellulose	5.61	6.37	0.88
21	2011	ITO/PEN	110 °C for 5 min	Graphite (1.6 g, 325 mesh, Alfa Aesar) + carbon black (0.4 g, Printex XE2, Degussa) + Sb-doped SnO_2 (0.4 g, Zelec ECP 3010-XC, Milliken chemicals) + 3-methoxypropionitrile (3 g) + poly(vinylidenefluoride-*co*-hexafluoropropylene) (9 g)	4.24	4.81	0.88

Table 2 Reported carbon counter electrodes for DSCs prepared by screen-printing method (CNT: carbon nanotube, DWCNT: double-wall carbon nanotube, FTO: F-doped SnO_2, ITO: indium tin oxide).

Ref. number	Year	Substrates	Annealing conditions	Materials	Photoenergy conversion efficiency of carbon (or Pt) counter electrodes (%)		
					Carbon (C)	Pt	Ratio: (C)/(Pt)
22	2000	Porous TiO_2/ZrO_2 electrode (monolithic structure)	No details (in refs.)	Graphite powder (Alpha 641) + amorphous carbon (Printex-L, Degussa) + α-terpineol + titanium alkoxide	No data	No data	–
23	2001	Porous TiO_2/ZrO_2 electrode (monolithic structure)	450 °C for 2 h	No details (in refs. [1,22])	No data	No data	–
24	2003	Porous TiO_2/ZrO_2 electrode (monolithic structure)	450 °C for 2 h	No details (in ref. [23])	No data	No data	–

(*continues on next page*)

Table 2 (*Continued*).

Ref. number	Year	Substrates	Annealing conditions	Materials	Photoenergy conversion efficiency of carbon (or Pt) counter electrodes (%)		
					Carbon (C)	Pt	Ratio: (C)/(Pt)
25	2007	FTO/glass	100 °C over night	Hard carbon spherules (75 wt %, made from sugar: HCS-1) + carbon black (20 wt %, d = 30 nm) + poly(vinylidene fluoride) (5 wt %) in *N*-methyl-2-pyrrolidone (as printing solvent)	4.7	6.5	0.72
				Hard carbon spherules (75 wt %, made from sugar: HCS-2) + carbon black (20 wt %, d = 30 nm) + poly(vinylidene fluoride) (5 wt %) in *N*-methyl-2-pyrrolidone (as printing solvent)	5.7	6.5	0.88
				Carbon black (d = 30 nm) + poly(vinylidene fluoride) in *N*-methyl-2-pyrrolidone (as printing solvent)	5.7	6.5	0.88
				Graphite + carbon black (20 wt %, d = 30 nm) + TiO_2 (in ref. [1])	3.8	6.5	0.58
26	2010	Silver layer/ alumina ceramics substrate	150 °C for 1 h	Carbon + epoxy resin + hardener + ei(ethylene glycol) methyl ether	1.2	1.8	0.67
27	2010	No details	No details	CNT ink (ref. [*Physica B* **323**, 71 (2002)])	8.03	8.8	0.91
28	2010	FTO/glass	300 °C for 15 min	DWCNT (d = 5 nm, L = 20 μm, Sc = 450 m^2/g) + ethyl cellulose + α-terpineol	6.05	6.8	0.89
29	2010	FTO/glass	350 °C for 10 min + at 430 °C for 20 min	CNT (10 % in ink) + α-terpineol + ethyl cellulose + polymer surface modifier (HSPM, 5 %)	5.94	7.15	0.83
				CNT (10 % in ink) + α-terpineol + ethyl cellulose ink)	5.69	7.15	0.80

Table 3 Reported carbon counter electrodes for DSCs prepared excluding doctor-blading and screen-printing methods (CNT: carbon nanotube, DWCNT: double-wall carbon nanotube, MWCNT: multi-wall carbon nanotube, SWCNT: single-wall carbon nanotube, *d*: diameter, *L*: length, *t*: thickness, Sc: specific surface area, FTO: F-doped SnO_2, ITO: indium tin oxide, PVDF: poly(vinylidene fluoride), HFP: hexafluoropropene, PEDOT: poly(3,4-ethylenedioxythiophene, PSS: poly(styrene sulfonate), CVD: chemical vapor deposition).

Ref. number	Year	Preparation method	Substrates	Annealing conditions	Materials	Photoenergy conversion efficiency of carbon (or Pt) counter electrodes (%)		
						Carbon (C)	Pt	Ratio: (C)/(Pt)
13	2009	–	Flexible graphite sheets (t = 0.2 mm, density = 0.03 g/m^2)	–	flexible graphite sheets (t = 0.2 mm, density = 0.03 g/m^2)	2.88	6.37	0.45
20	2010	Spray	FTO/glass	No details	CNT micro-balls + ethanol	5.54	6.37	0.87
27	2010	CVD	TCO glass (not clear)	Processed at 550 °C	CNTs on FTO substrates	10.04	8.8	1.14
30	2003	Drop casting	FTO/glass	60 °C	SWCNT (20 mg) + water (50 mL)	3.5	5.4	0.65
					Carbon filament (20 mg) + water (50 mL)	2.5	5.4	0.46
					Nanohorn carbon (20 mg) + water (50 mL)	2.4	5.4	0.44
		Filtration	Teflon membrane filter	60 °C	SWCNT (20 mg) + water (50 mL), filtered by a Teflon membrane filter	4.5	5.4	0.83
					SWCNT (20 mg) + water (50 mL), filtered by a Teflon membrane filter	0.2	5.4	0.04
					SWCNT (20 mg) + water (50 mL), filtered by a Teflon membrane filter	0.04	5.4	0.01
31	2006	Spray	FTO/glass	100 °C on substrate	Graphite powder (0.8 g, 325 mesh, Alpha Aesar) + amorphous carbon (0.2 g, Printex-L, Degussa) + TiO_2 (1 g, P25, Degussa) + ethanol (5 g). Mixture stirred vigorously for 12 h before use.	5	No data	No data
32	2007	Dip coating	FTO/glass	80 °C for 30 min	PEDOT: PSS (in DMSO) + carbon black (0.1 wt %)	5.81	5.66	1.03
33	2006	Sandwiched between working and counter electrodes	Dyed-porous TiO_2 electrodes and FTO/glass	No annealing	Polyaniline-loaded carbon black (30 mg) + 1,3-diethleneoxide derivative of imidazolium iodide (250 mg) (carbon/electrolyte composite)	3.48	No data	–
34	2007	Sandwiched between working and counter electrodes	Dyed-porous TiO_2 electrodes and FTO/glass	No annealing	SWCNT (30 mg) + 1,3-diethleneoxide derivative of imidazolium iodide (400 mg) (SWCNT/electrolyte composite)	2.3	No data	–

(*continues on next page*)

Table 3 (*Continued*).

Ref. number	Year	Preparation method	Substrates	Annealing conditions	Materials	Photoenergy conversion efficiency of carbon (or Pt) counter electrodes (%)		
						Carbon (C)	Pt	Ratio: (C)/(Pt)
35	2008	CVD	FTO/glass	No details (in references)	Raw SWCNT	0.57	1.49	0.38
		Transfer of free-standing film	FTO/glass	No details	Purified SWCNT obtained by oxidation (at 450 °C for 1 h in air) and rinsing with 37 % HCl	1.46	1.49	0.98
		Coating	FTO/glass	Dry	MWCNT (in HCl at 50 °C for 12 h, in H_2SO_4/HNO_3 (3:1) at 50 °C for 10 min, on polypropylene filter paper by filtration, and on FTO/glass)	0.62	1.49	0.42
		CVD + transfer	FTO/glass	Dry	DWCNT	0.45	1.49	0.30
		Brush coating	FTO/glass	110 °C for 5 min	Carbon black (80 wt %, Black Pearl 2000) + PDVDF-HFP (20 wt %) in *N*-methyl-2-pyrrolidone	0.08	1.49	0.05
					Carbon black (80 wt %, Vulcan XC 72, Cabot Co.) + PDVDF-HFP (20 wt %)	0.18	1.49	0.12
					Carbon black (80 wt %, Pred Materials Inc., Japan) + PDVDF-HFP (20 wt %)	0.11	1.49	0.07
36	2008	No details	ITO/glass	150 °C for 1 h	Activated carbon (Sc = 36 m^2/g) + carbon black + water + ethanol + carboxymethyl cellulose + TiO_2 + NH_3 aq.	2.589	No data	–
37	2008	Spray	FTO/glass	120 °C substrate	MWCNT (d = 30 nm, 100 mg) + ethanol (100 mL)	7.59	No data	–
38	2008	Spin coat	FTO/glass	110 °C for 30 min	MWCNT (1.35 %, d = 10–15 nm, L = 0.1–10 μm) + PEDOT:PSS	6.5	8.5	0.76
					MWCNT (1.35 %, d = 10–15 nm, L = 0.1–10 μm) + PSSA	3.6	8.5	0.42
39	2009	No details	TCO glass (not clear)	No details	No details	No data	No data	No data
40	2009	In the reference	No details	No details	No details (in ref. [9])	1.04 %	No data	No data
41	2009	Dip coating	FTO/glass	80 °C for 30 min	Carbon black (0.2 wt %) + DMSO/PEDOT:PSS (1/3)	5.24	No data	–
42	2009	Spin coating	FTO/glass	80 °C for 30 min.	PEDOT: PSS (1:3 wt % dispersion in water) + DMSO + carbon black (0.2 wt %)	4.1	No data	–

(*continues on next page*)

Table 3 (*Continued*).

Ref. number	Year	Preparation method	Substrates	Annealing conditions	Materials	Photoenergy conversion efficiency of carbon (or Pt) counter electrodes (%)		
						Carbon (C)	Pt	Ratio: (C)/(Pt)
43	2009	Dip coating	Fiber-structured DSC photoelectrode	No details	Graphite (1.4 g) + carbon black (0.4 g, Printex XE2, Degussa) + TiO_2 (0.72 g, P25, Degussa) + 3-methoxypropionitrile (2 g + 10 g) + PDVF-HFP (5 wt %)	0.0000537	No data	–
44	2009	Electrophoration	FTO/glass	450 °C for 1 h	MWCNT (0.02 g) + $Mg(NO_3)_2$ (0.005 g) + methanol (60 mL)	1.08	No data	–
45	2009	Spin coat	FTO/glass	250 °C for 1 h.	Carbon particle (650 mg, $d < 50$ nm, Sc > 100 m^2/g) + TiO_2 colloid (P25, 1 mL, 20 wt %) + water (2 mL) + Triton X-100 (1 mL)	5.5	6.4	0.86
46	2010	Spin coat	ITO/glass	120 °C for 5 min	EDOT (40 µL) + iron (III) toluenesulfonate (0.434 g) + imidazole (0.05g) + MWCNT (0.6 wt % by PEDOT) [resulting in poly(3,4-ethylenedioxythiophene) films]	8.08	7.77	1.04
47	2010	No details	Silicon substrate (35 µm)	No details	MWCNT (t = 35 µm)	2.53	4.9	0.52
48	2010	Soot staining method	TCO glass (not clear)	No details	Soot staining	0.9	1.5	0.60
49	2010	Polymerized	Flexible graphite paper	40 °C for 6 h	Polyaniline	7.36	7.45	0.99
		–	Flexible graphite paper	–	Flexible graphite paper	3.84	7.45	0.52
50	2010	Spray	FTO/glass	Hot substrates at 120 °C	Ferrocene-derivatized large pore size mesoporous carbon (6 mg) + ethanol (6 mL)	7.89	No data	–
					Large pore size mesoporous carbon (6 mg) + ethanol (6 mL)	7.03		
					Nano-sized carbon (6 mg, Valcan) + ethanol (6 mL)	6.77		
51	2010	Sliced oak wood	Free standing	900 °C for 4 h in Ar	Sliced highly ordered mesoporous carbon arrays (carbonized oak)	7.98	7.93	1.01
		Sliced bamboo	Free standing	900 °C for 4 h in Ar	Sliced highly ordered mesoporous carbon arrays (carbonized bamboo)	4.53	7.93	0.57

(*continues on next page*)

Table 3 (*Continued*).

Ref. number	Year	Preparation method	Substrates	Annealing conditions	Materials	Photoenergy conversion efficiency of carbon (or Pt) counter electrodes (%)		
						Carbon (C)	Pt	Ratio: (C)/(Pt)
52	2010	Spray	FTO/glass	No details	Large pore size mesoporous carbon (no details)	8.18	8.85	0.92
					CMK-3 carbon (no details)	6.75	8.85	0.76
					Vulcan carbon (no details)	6.77	8.85	0.76
53	2010	Drop casting	FTO/glass	Hot substrates at 150 °C	SWCNT (2 mg) + water (10 mL)	2.5	4.5	0.56
			Stainless steel			3.92	4.5	0.87
54	2010	Spin coating	FTO/glass	Heated at 350 °C in air for 2 h.	Graphene + triblock copolymer + polyethylene oxide in water	4.99	5.48	0.91
55	2011	Transfer (after drop casting and CVD)	FTO/glass	No details	Graphene (drop casting) + MWCNT (CVD)	3	No data	–
56	2011	Drop casting	FTO/glass	Drying at room temperature	Graphene + 2-propanol +	5.73	6.89	0.83

For the carbon counter electrodes in DSCs, one of the main preparation methods is doctor-blading. Hence, at first, the results of DSCs by doctor-blade coating methods are shown in Table 1. At the beginning, the research focused on carbon counter electrodes for monolithic-structured DSCs without platinum [1,2]. Kay and Grätzel reported a conversion efficiency of 6.67 %, confirmed by the National Renewable Energy Laboratory (NREL) [1]. In 2003, a study where a fluorine-doped tin oxide (FTO)/glass substrate was coated with carbon counter electrodes for DSCs was published with a conversion efficiency ratio of 0.90 [3]. More recently, conversion efficiencies of 9.1 % (in 2006) [4] and 9.15 % (in 2008) [7] were reported by doctor-blading methods.

Second, as an important preparation method, the results of screen-printing methods have been summarized in Table 2. Comparing the progress of the doctor-blading method (in Table 1), the publication number about screen-printing method is smaller, which implies the necessity of a special technique and knowledge of the screen-printing method. Screen-printing deposition is the method suitable for the industrial production of carbon counter electrodes for DSCs. Other methods deposit the carbon ink over the whole substrate, and then the electrode must be formed from the ink layer through either scratching or photolithography resist polymers. There are two types of carbon ink: water-based and screen-printing oil-based carbon ink. Water-based carbon ink can flow over the side of the printed area, thus accurate printing is difficult with this technique (Fig. 2, right-hand side), while screen printing deposits the oil-based carbon ink accurately (Fig. 2, left-hand side), which makes it attractive for the cost-effective fabrication of DSCs.

As a group of minor methods (excluding doctor-blading and screen printing), the DSCs results are summarized in Table 3. In order to deposit carbon materials on a conducting substrate, a coating process is necessary. Carbon inks are used for printing techniques, including: spray [20,31,37,50,52], spin coating [38,42,45,46,54], dip coating [32,41,43], drop casting [30,53,56], polymerization [49], and sandwiching mixed with electrolyte [33,34]. On the other hand, chemical vapor deposition (CVD) [27,35], transfer methods [35,55], soot staining [48] electroporation [44], and filtration [30] are not printing processes, and do not require inks.

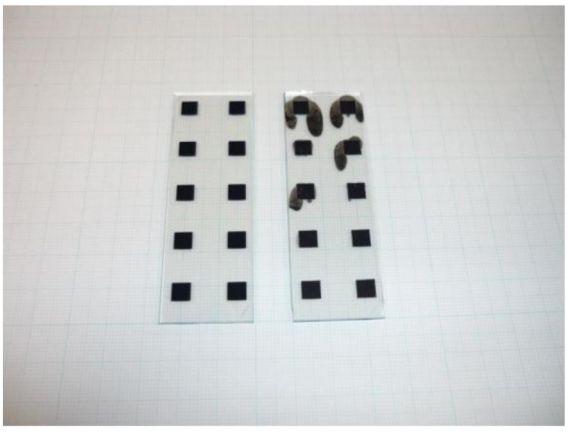

Fig. 2 Screen-printed porous carbon layers using terpineol-based ink (left) and water-based ink (right).

In each method above, an annealing process has also been investigated for activating and fixing the carbon layers, where the binding polymers were removed by oxidation at temperatures over 400 °C. The carbon particles are only weakly bonded together; therefore, metal oxide particles, such as TiO_2 [1,4,7,11,12,17,18,22,23,25,31,36,43,45] and SnO_2 [13,14,21], have been used to improve the adhesion. As no annealing methods, on the other hand, the carbon particles on the DSC counter electrodes are coated with electron or ion conducting polymers, which help the particle adhesion and the electronic conduction from substrate to carbon particles [25,26,32,35,38,41,42,43,46].

High conversion efficiencies over 8 % were published using carbon counter electrodes [4,7,27,46,52]. Despite the extensive research in this area, the other reported conversion efficiencies are less than 8 %. The lower efficiency is because of the quality of the other components in the DSC: the ruthenium dye, the electrolyte, the nanocrystalline-TiO_2 electrode, and the FTO/glass substrate. Moreover, the solar cell assembly technique is also important for making high-efficiency DSCs. Additionally, the low conversion efficiency of natural DSCs with has been improved using a carbon nanotube (CNT) counter electrode [35,48].

Basically, FTO/glass plates were utilized for substrates of carbon counter electrodes. Stainless steel has also been used for carbon counter electrode conduction substrates with promising results [7,53]. Sliced oak and bamboo were carbonized to form active carbon substrates and used in DCSs [51]. The oak-derived carbon electrode was better than the bamboo-derived one and produced higher conversion efficiency than platinum counter electrodes. Sheets of flexible graphite paper have also been used as a conducting and catalytic material; although the flexible graphite paper electrode did not demonstrate high efficiency, it was improved by adding polyaniline to the surface [49]. Although the carbonized wood [51] and the flexible graphite paper with polyaniline [49] showed high efficiency, these materials were not suitable for the DSC electrolyte because of their porous structures, in order to encapsulate the electrolyte in DSCs. Hence, nonporous materials like glass or metal substrates are required for DSCs.

Although recent advances in CNT fabrication methods have lowered their production cost, they are still too expensive for DSCs. Carbon particles are a cheaper alternative; these materials include carbon, carbon particles, carbon black, graphite, active carbon, and mesoporous carbon. Carbon black and active carbon are the same amorphous carbon material, made by the pyrolysis of acetylene. However, graphite is highly crystalline carbon, created at high temperatures around 1000 °C. Active carbon and mesoporous carbon are highly porous materials. The former is a natural material, and the latter contains both artificial and natural materials. Graphene [54–56], carbonized woods [51], and flexible graphite paper [13,49] are carbon materials with unique properties. Graphene is a single atomic layer of graphite,

which was first discovered by Geim and Novoselov, who won the Nobel Prize in Physics in 2010 for their work. Graphene has produced promising results for DSC counter electrodes [54,56].

In spite of the variety of fabrication methods for carbon counter electrodes in DSCs, the screen-printing method is promising because of the fixation of printed carbon position (Fig. 2) and the high-speed coating process. However, no details of the screen-printing technique have yet been published. In this paper, we describe the fabrication of DSC carbon counter electrodes using the screen-printing method, and evaluate their performance.

EXPERIMENTAL

Chemicals and materials

F-doped SnO_2 coated glass (FTO/glass) for the photoelectrodes (SOLAR, t = 4.0 mm, 9.5 Ω/□) and counter electrodes (TEC15, t = 2.2 mm, 15 Ω/□) was supplied by Nippon Sheet Glass Co. Ltd. These substrates were cleaned by sonication in acetone. The TiO_2 nanocrystalline anatase inks for the transparent dye coated layer (PST-18NR, particle size: 18 nm) and for the light scattering layer (PST-400C, particle size: 400 nm) were purchased from JGC-CCIC (Japan). The Ru complex dye, *cis*-diisothiocyanato-bis(2,2'-bipyridyl-4,4'-dicarboxylato)ruthenium(II) bis(tetrabutylammonium) (N-719), was purchased from Solaronix SA (Switzerland). The N-719 dye was adsorbed from a 0.5 mM solution in acetonitrile and *tert*-butyl alcohol (1:1, v/v). The electrolyte was a solution of 0.60 M 1-methyl-3-propylimidazolium iodide, 0.03 M I_2, 0.10 M guanidinium thiocyanate, and 0.50 M 4-*tert*-butylpyridine in acetonitrile and valeronitrile (85:15, v/v). The 1-methyl-3-propylimidazolium iodide was synthesized as previously described [58].

Preparation of carbon layer printing ink

The TiO_2 colloid was prepared as previously reported [4]: $Ti[OCH(CH_3)_2]_4$ (12.5 mL) in isopropanol (2 mL) was added dropwise to water (75 mL) with stirring. Nitric acid 65 % (0.6 mL) was added, and the solution heated at 80 °C for 8 h, and then the TiO_2 precipitate was peptized to form a white, transparent colloid. The fabrication scheme for the screen-printing of carbon inks is shown in Fig. 3.

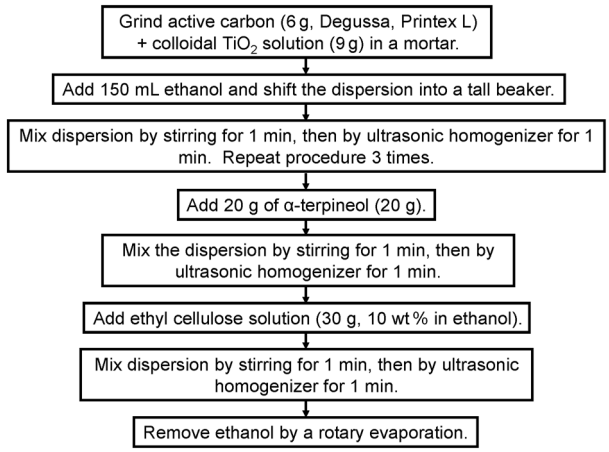

Fig. 3 Preparation scheme of screen-printing carbon ink for counter electrodes in DSCs.

The TiO_2 colloidal solution (9 mL) was then added dropwise to carbon powder (6 g) (Printex L, Degussa) and ground in an alumina mortar. Ethanol was added dropwise to the carbon. The carbon dispersion in the mortar was transferred to a tall beaker using ethanol (150 mL) and stirred (4 cm magnet tip, 300 rpm). The ultrasonic homogenization was performed using a Ti-horn-equipped sonicator (Vibra cell, Bioblock Scientific). α-Terpineol and a mixture of two ethanol solutions containing different types of ethyl cellulose (#E0265 and #E0266, 50/50 w/w, Tokyo Chemical Industry, Japan) were added, and then stirred and sonicated. The dispersion was concentrated under vacuum to give the printing ink for the carbon counter electrodes.

Preparation of counter electrodes

A hole (1 mm diameter) was drilled in the FTO glass (TEC 15 Ω/□, 2.2 mm thickness, Nippon Sheet Glass, Japan) by drilling. The perforated sheet was washed with H_2O, then 0.1 M HCl solution in ethanol and cleaned by ultrasound in an acetone bath for 10 min. The carbon ink was screen-printed onto the cleaned FTO/glass substrate then heated at 450 °C for 15 min, resulting in a porous carbon counter electrode. After heating, the thickness of the carbon layer was measured using a surface profilometer.

The Platinum catalyst was deposited on the FTO glass by coating with a drop of H_2PtCl_6 solution (2 mg Pt in 1 mL ethanol) and then heated at 400 °C for 15 min [59].

Preparation of the mesoporous TiO_2 layer [59]

FTO glass (Solar 4 mm thickness, 10 Ω/□, Nippon Sheet Glass, Japan) was first cleaned in a detergent solution using an ultrasonic bath for 15 min, and then rinsed with water and ethanol. After treatment in a UV-O_3 system for 18 min, the FTO glass plates were immersed in a 40 mM aqueous $TiCl_4$ solution at 70 °C for 30 min and washed with water and ethanol. A layer of ink (PST-18NR) was screen-printed onto the FTO glass plate, allowed to relax for 3 min to reduce the surface irregularity and then dried for 6 min at 125 °C. This screen-printing procedure was repeated until a thickness of 12–14 μm was achieved for the working electrode. After drying the films at 125 °C, two layers of TiO_2 ink (PST-400C, JGC-CCIC, Japan) were deposited by screen-printing, resulting in a light-scattering TiO_2 film containing 400-nm-sized anatase particles of 4–5 μm thickness. The electrodes were gradually heated under an airflow at 325 °C for 5 min, at 375 °C for 5 min, at 450 °C for 15 min, and finally at 500 °C for 15 min. The TiO_2 double-layer film thus produced was treated again with 40 mM $TiCl_4$ solution, then rinsed with water and ethanol and sintered at 500 °C for 30 min. After cooling to 80 °C, the TiO_2 electrode was immersed in 0.5 mM N-719 dye solution in acetonitrile and *tert*-butyl alcohol (1:1 v/v) and kept at room temperature for 20–24 h to assure complete sensitizer uptake.

Assembly of the DSC [59]

The dye-covered TiO_2 electrode and the counter electrode were assembled into a sandwich-type cell (Fig. 1) and sealed with a 25 μm hot-melt gasket made of the ionomer Surlyn 1702 (DuPont). The TiO_2 electrodes used were 0.25 cm^2 (5 × 5 mm). The aperture of the Surlyn frame was 2 mm larger than that of the TiO_2 area, and its width was 1 mm. The hole in the counter electrode was sealed by a film of Bynel 4164 (DuPont) using a hot iron bar covered with a fluorine polymer film. A hole was then made in the Bynel film with a needle. A drop of the electrolyte was put in the hole in the back of the counter electrode, and it was introduced into the cell via vacuum backfilling. The cell was placed in a vacuum, and subsequent exposure to ambient pressure pushed the electrolyte into the cell. The hole was then sealed using a hot-melt ionomer film (Bynel 4164, 35 μm, DuPont) and a cover glass (0.1 mm). Solder

(Cerasolza, Asahi Glass) was applied to each side of the FTO electrodes, 1 mm away from the edge of the Surlyn gasket and hence 4 mm from the photoactive TiO_2 layer. Light reflection losses were eliminated using black plastic tapes on the DSC surface to reduce the scattered light.

Measurements of photocurrent–voltage curves and impedance spectra

Photocurrent–voltage characteristics were measured with a source meter (ADCMT, Japan) under illumination from a solar simulator consisting of a xenon arc lamp (450 W) and AM 1.5 glass filters (Yamashita Denso, Japan). Light intensity was calibrated with a silicon photodiode (Bunkou Keiki, Japan). Light-shading masks were attached to the DSCs in order to reduce scattered light from the edge of the glass electrodes of the dye-modified TiO_2 layer [60].

RESULTS AND DISCUSSION

Appearance and morphology of screen-printed carbon layers

Figure 2 shows the screen-printed carbon layers. The layers deposited using α-terpineol-based solvent, remained in the correct position. However, the water-based carbon ink [4] flows to the side of the printed area.

Figure 4 shows SEM images of the screen-printed carbon layers using α-terpineol-based inks and water-based inks. In the low-magnification view (× 150), the α-terpineol-based ink carbon layers were smooth with no big aggregates (Fig. 4a). However, the water-based ink carbon layers contained large aggregates, up to 100 μm in diameter (Fig. 4b), which are visible to the naked eye. In the high-resolution view (×30 000), the surface of α-terpineol-based ink carbon layer was again smoother than that of the water-based ink. Therefore, the water-based ink contained large (~100 μm) and small (~0.5 μm) aggregates, which were not observed in the α-terpineol-based ink carbon layer.

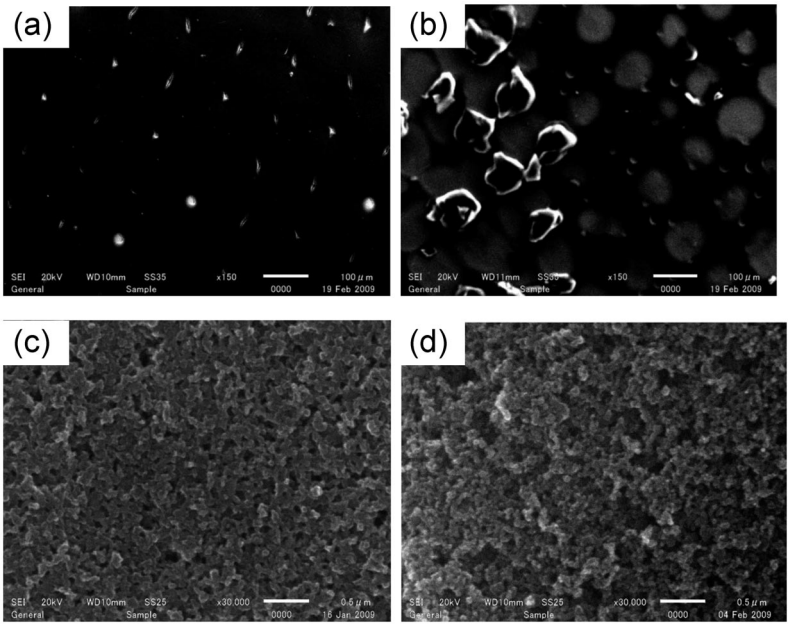

Fig. 4 SEM images of printed carbon layers at ×150 magnification using terpineol (a) and water- based ink (b), and images at ×30 000 magnification using terpineol (c) and water-based (d) ink.

DSC photovoltaic results using screen-printed carbon counter electrodes

Figure 5 shows the variation of photovoltaic parameters with the thickness of the DSC carbon counter electrodes: the short-circuit photocurrent density (J_{SC}) (a); the open-circuit photovoltage (V_{OC}) (b); the fill factors (*FF*) (c); the photoenergy conversion efficiency (η) (d). Increasing the thickness of the carbon counter electrodes increased J_{SC} and decreased V_{OC}, although the size of the variation was not significant. The variation of *FF* with the carbon-electrode thickness was large (Fig. 5c); *FF* increased from 0.4 to 0.6 as the carbon-electrode thickness increased, and resulted in η from 4 to 7 %. The peak value of η was obtained at a carbon-electrode thickness of 15 μm for both α-terpineol-based ink and water-based ink [4].

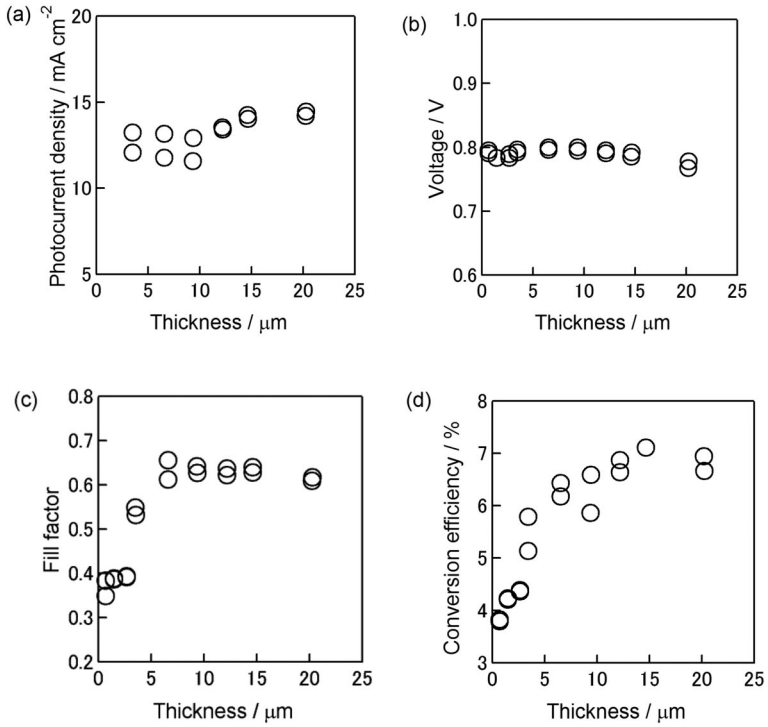

Fig. 5 Photovoltaic characteristics of DSCs with variations in the thickness of the porous-carbon catalyst layers on FTO/glass counter electrodes: (a) short-circuit photocurrent density, (b) open-circuit photovoltage, (c) fill factor, and (d) and energy conversion efficiency.

Figure 6 shows photocurrent–voltage curves for DSCs with a screen-printed carbon counter electrode and with a platinum counter electrode. The thickness of the carbon counter electrode was 15 μm. The photovoltaic parameters are summarized in Table 4. The resulting conversion efficiencies of carbon and platinum were 7.11 and 6.94 %, respectively. The conversion ratio (C/Pt) was 1.02, which is one of the highest ratios reported for carbon counter electrodes in DSCs.

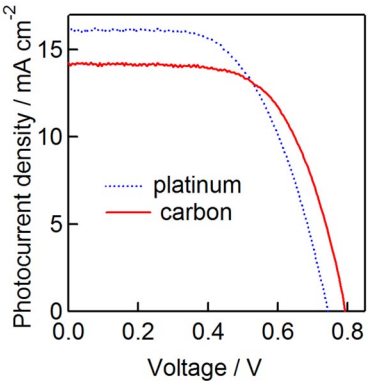

Fig. 6 Photocurrent–voltage curves of DSCs with two types of counter electrodes: platinum and terpineol-based carbon.

In conclusion, screen-printed carbon black is a promising catalyst for DSC counter electrodes. We report the first detailed account of the fabrication process of carbon counter electrodes by the screen-printing method. By optimizing the film thickness, a conversion efficiency ratio (C/Pt) of 1.02 and a conversion efficiency of 7.11 % were obtained.

Table 4 Photovoltaic parameters of DSCs using platinum and carbon counter electrodes.

Catalyst material	J_{SC}/mA cm^{-2}	V_{OC}/V	*FF*	η/%
Platinum	16.2	0.743	0.576	6.94
Carbon	14.2	0.792	0.630	7.11

REFERENCES

1. A. Kay, M. Grätzel. *Sol. Energy Mater. Sol. Cells* **44**, 99 (1996).
2. N. Papageorgiou, P. Liska, A. Kay, M. Grätzel. *J. Electrochem. Soc*. **146**, 898 (1999).
3. K. Imoto, K. Takahashi, T. Yamaguchi, T. Komura, J. Nakamura, K. Murata. *Sol. Energy Mater. Sol. Cells* **79**, 459 (2003).
4. T. N. Murakami, S. Ito, Q. Wang, M. K. Nazeeruddin, T. Bessho, I. Cesar, P. Liska, R. Humphry-Baker, P. Comte, P. Péchy, M. Gtätzel. *J. Electrochem. Soc.* **153**, A2255 (2006).
5. E. Ramasamy, W. J. Lee, D. Y. Lee, J. S. Song. *Appl. Phys. Lett.* **90**, 173103 (2007).
6. H. F. Hossain, S. Biswas, T. Takahashi, Y. Kubota, A. Fujishima. *Thin Solid Films* **516**, 7149 (2008).
7. T. N. Murakami, M. Grätzel. *Inorg. Chim. Acta* **361**, 572 (2008).
8. W. J. Lee, E. Ramasamy, D. Y. Lee, J. S. Song. *J. Photochem. Photobiol., A* **194**, 27 (2008).
9. M. F. Hossain, S. Biswas, T. Takahashi. *Thin Solid Films* **517**, 1294 (2008).
10. W. J. Lee, E. Ramasamy, D. Y. Lee, J. S. Song. *Sol. Energy Mater. Sol. Cells* **92**, 814 (2008).
11. S. Peng, F. Cheng, J. Shi, J. Liang, Z. Tao, J. Chen. *Solid State Sci.* **11**, 2051 (2009).
12. G. Wang, W. Xing, S. Zhuo. *J. Power Source* **194**, 568 (2009).
13. J. Chen, K. Li, Y. Luo, X. Guo, D. Li, M. Deng, S. Huang, Q. Meng. *Carbon* **47**, 2704 (2009).
14. K. Li, Y. Luo, Z. Yu, M. Deng, D. Li, Q. Meng. *Electrochem. Commun.* **11**, 1346 (2009).
15. P. Li, J. Wu, J. Lin, M. Huang, Y. Huang, Q. Li. *Sol. Energy* **83**, 845 (2009).

16. B. Fang, S.-Q. Fan, J. H. Kim, M.-S. Kim, M. Kim, N. K. Chaudhari, J. Ko, J.-S. Yu. *Langmuir* **26**, 11238 (2010).
17. L. L. Chen, J. Liu, J. B. Zhang, X. W. Zhou, X. L. Zhang, Y. Lin. *Chin. Chem. Lett.* **21**, 1137 (2010).
18. G. Wang, L. Wang, W. Xing, S. Zhuo. *Mater. Chem. Phys.* **123**, 690 (2010).
19. G. Li, F. Wang, Q. Jinag, X. Gao, P. Shen. *Angew. Chem., Int. Ed*. **49**, 3653 (2010).
20. S. I. Cha, B. K. Koo, S. H. Seo, D. Y. Lee. *J. Mater. Chem.* **20**, 659 (2010).
21. K. Miettunen, M. Toivola, G. Hashmi, J. Salpakari, I. Asghar. *Carbon* **49**, 528 (2011).
22. S. Burnside, S. Winkel, K. Brooks, V. Shklover, M. Grätzel, A. Hinsch, R. Kinderman, C. Bradbury, A. Hagfeldt, H. Pettersson. *J. Mater. Sci.: Mater. Electron.* **11**, 355 (2000).
23. H. Pettersson, T. Gruszecki. *Sol. Energy Mater. Sol. Cells* **70**, 203 (2001).
24. H. Pettersson, T. Gruszecki, L.-H. Johansson, P. Johander. *Sol. Energy Mater. Sol. Cells* **77**, 405 (2003).
25. Z. Huang, X. Liu, K. Li, D. Li, Y. Luo, H. Li, W. Song, L. Chen, Q. Meng. *Electrochem. Commun.* **9**, 596 (2007).
26. F. Ghamouss, R. Pitson, F. Odobel, M. Boujtita, S. Caramori, C. A. Bignozzi. *Electrochim. Acta* **55**, 6517 (2010).
27. J. G. Nam, Y. J. Park, B. S. Kim, J. S. Lee. *Scripta Mater.* **62**, 148 (2010).
28. D. W. Zhang, X. D. Li, S. Chen, F. Tao, Z. Sun, X. J. Yin, S. M. Huang. *J. Solid State Electrochem.* **14**, 1541 (2010).
29. H. J. Choi, J. E. Shin, G.-W. Lee, N.-G. Park, K. Kim, S. C. Hong. *Curr. Appl. Phys*. **10**, S165 (2010).
30. K. Suzuki, M. Yamaguchi, M. Kumagai, S. Yanagida. *Chem. Lett*. **32**, 28 (2003).
31. J. Halme, M. Toivola, A. Tolvanen, P. Lund. *Sol. Energy Mater. Sol. Cells* **90**, 872 (2006).
32. J.-G. Chen, H.-Y. Wei, K.-C. Ho. *Sol. Energy Mater. Sol. Cells* **91**, 1472 (2007).
33. N. Ikeda, K. Teshima, T. Miyasaka. *Chem. Commun.* 1733 (2006).
34. N. Ikeda, T. Miyasaka. *Chem. Lett.* **36**, 466 (2007).
35. H. Zhu, H. Zeng, V. Subramanian, C. Masarapu, K.-H. Hsuan, B. Wei. *Nanotechnology* **19**, 465204 (2008).
36. H. S. Lee, H. Y. Lee, S. Y. Ahn, K. H. Kim, J. Y. Kwon. *Adv. Mater. Res.* **31**, 176 (2008).
37. E. Ramasamy, W. J. Lee, D. Y. Lee, J. S. Song. *Electrochem. Commun.* **10**, 1087 (2008).
38. B. Fan, X. Mei, K. Sun, J. Ouyang. *Appl. Phys. Lett.* **93**, 143103 (2008).
39. N. Kato, Y. Takeda, K. Higuchi, A. Takeichi, E. Sudo, H. Tanaka, T. Motohiro, T. Sano, T. Toyoda. *Sol. Energy Mater. Sol. Cells* **93**, 893 (2009).
40. H. F. Hossain, T. Takahashi, S. Biswas. *Electrochem. Commun.* **11**, 1756 (2009).
41. P. Balraju, P. Suresh, M. Kumar, M. S. Roy, G. D. Sharma. *J. Photochem. Photobiol., A* **206**, 53 (2009).
42. P. Balraju, M. Kumar, M. S. Roy, G. D. Sharma. *Synth. Met.* **159**, 1325 (2009).
43. M. Toivola, M. Ferenets, P. Lund, A. Harlin. *Thin Solid Films* **517**, 2799 (2009).
44. S. Pimanpang, W. Maiaugree, W. Jarernboon, S. Maensiri, V. Amornkitbamrung. *Synth. Met.* **159**, 1996 (2009).
45. P. Joshi, Y. Xie, M. Ropp, D. Galipeau, S. Bailey, Q. Qiao. *Energy Environ. Sci*. **2**, 426 (2009).
46. K.-M. Lee, W.-H. Chiu, H.-Y. Wei, C.-W. Hu, V. Suryanarayanan, W. F. Hsieh, K.-C. Ho. *Thin Solid Films* **518**, 1716 (2010).
47. X. Li, H. Lin, Y. Zhang. *Chem. Lett.* **39**, 40 (2010).
48. M. H. Bazargan. *Int. J. Chem. Tech. Res.* **2**, 615 (2010).
49. H. Sun, Y. Luo, Y. Zhang, D. Li, Z. Yu, K. Li, Q. Meng. *J. Phys. Chem. C* **114**, 11673 (2010).
50. E. Ramasamy, J. Lee. *Carbon* **48**, 3715 (2010).
51. Q. W. Jiang, G. R. Li, F. Wang, X. P. Gao. *Electrochem. Commun.* **12**, 924 (2010).
52. E. Ramasamy, J. Lee. *Chem. Commun*. **46**, 2136 (2010).

53. G. Calogero, F. Bonaccorso, O. M. Maragò, P. G. Gucciardi, G. Di Marco. *Dalton Trans.* **39**, 2903 (2010).
54. J. D. Roy-Mayhew, D. J. Bozym, C. Punckt, I. A. Aksay. *ACS Nano* **4**, 6203 (2010).
55. H. Choi, H. Kim, S. Hwang, W. Choi, M. Jeon. *Sol. Energy Mater. Sol. Cells* **95**, 323 (2011).
56. L. Kavan, J. H. Yum, M. Grätzel. *ACS Nano* **5**, 165 (2011).
57. Y. Saito, T. Kitamura, Y. Wada, S. Yanagida. *Chem. Lett.* **31**, 1060 (2002).
58. P. Bonhôte, A. P. Dias, M. Armand, N. Papageorgiou, K. Kalyanasundaram, M. Grätzel. *Inorg. Chem.* **35**, 1168 (1996).
59. S. Ito, T. N. Murakami, P. Comte, P. Liska, C. Grätzel, M. K. Nazeeruddin, M. Grätzel. *Thin Solid Films* **516**, 4613 (2008).
60. S. Ito, M. K. Nazeeruddin, P. Liska, P. Comte, R. Charvet, P. Péchy, M. Jirousek, A. Kay, S. M. Zakeeruddin, M. Grätzel. *Prog. Photovoltaics* **14**, 589 (2006).

